10-1993

An Analysis of Carrier Phase Jitter in an M-PSK Receiver Utilizing MAP Estimation

William Osborne
osborne@engr.siu.edu

Brian Kopp
New Mexico State University - Main Campus

Published in Osborne, W., & Kopp, B. (1993). An analysis of carrier phase jitter in an M-PSK receiver utilizing MAP estimation. IEEE Military Communications Conference, 1993. MILCOM '93. Conference record. 'Communications on the Move,' v.2, 465-470. doi: 10.1109/MILCOM.1993.408624

AN ANALYSIS OF CARRIER PHASE JITTER IN AN M-PSK RECEIVER UTILIZING MAP ESTIMATION

William Osborne and Brian Kopp
New Mexico State University, Las Cruces, New Mexico

Abstract

The use of 8 and 16 PSK TCM to support satellite communications in an effort to achieve more bandwidth efficiency in a power-limited channel has been proposed. This paper addresses the problem of carrier phase jitter in an M-PSK receiver utilizing the high SNR approximation to the maximum a posteriori estimation of carrier phase. In particular, numerical solutions to 8 and 16 PSK self-noise and the amplitude suppression factor in the loop are presented. The effect of changing SNR on the loop noise bandwidth is also discussed. This data is then used to compute variance of phase error as a function of SNR. Simulation data is used to verify these calculations. The results show that there is a threshold in the variance of phase error verse SNR curves that is a strong function of SNR and a weak function of loop bandwidth. The M-PSK variance thresholds occur at SNR's in the range of practical interest for the use of 8 and 16-PSK TCM. This suggests that phase error variance is an important consideration in the design of these systems.

Introduction

With the advent of higher order modulation schemes such as 8 and 16 phase shift keying (PSK) trellis-coded modulation (TCM) for use on power limited channels, it is prudent to discuss M-ary phase shift keying (M-PSK) receiver performance [1]. In particular, the jitter of the received carrier, a critical performance measure, can be evaluated to help set minimum limits on operational signal-to-noise ratios (SNR).

For this analysis the chosen receiver structure is the high SNR approximation to the maximum a posteriori (MAP) carrier tracking loop [2], shown in Figure 1. This loop is easily constructed in an M-PSK configuration and with M=4 is compatible with the industry standard quadrature phase shift key (QPSK) Costas cross-over loop. Further, the analysis of QPSK carrier jitter for this loop is available in the literature, providing a reference point for expanding the analysis to 8 and 16 PSK.

To compute the carrier jitter (variance of the phase error) an equation for the variance can be derived from the baseband model of the loop. Two components of the variance equation, the self noise and the amplitude suppression factor, must be found numerically as a function of SNR for 8 and 16 PSK. A third important factor in the equation, the loop bandwidth (BW), is a function of the amplitude suppression factor and thus also of SNR.

In the first part of this paper the equation for the phase error variance is derived. This is followed by a calculation of the equivalent noise variance in the loop which results in a determination of the self noise. It is shown that self noise can be neglected for SNR's which would be considered for practical operation. Next the amplitude suppression factor is calculated and then used to examine the changing loop noise bandwidth. The loop noise BW is shown to have high and low SNR asymptotes with a transition from the "design" loop noise BW to a narrower BW as the SNR decreases. Once all of the components of the phase error variance have been assembled the results are presented along with simulation data. In the concluding part of the paper the nature of the variance of phase error is discussed.

The variance is shown to be a weak function of loop noise BW and a strong function of SNR. There is a threshold region of SNR below which the variance grows much faster than the SNR decreases. This suggests a minimum SNR to use for each M-PSK scheme to allow acquisition, prevent cycle slipping, and minimize the impact of phase error variance on bit error rate (BER) performance of the system.

Phase Error Variance

The equation for the phase error variance is found by first deriving the linear baseband model for the loop. From the model a transfer function between the equivalent noise port and the voltage controlled oscillator (VCO) port can be determined. Using this transfer function to relate the power spectral densities (PSD) of the loop equivalent noise to that of the phase error, the variance of the phase error can be determined. This approach parallels that of Hinedi and Lindsey [3].

The first step, deriving the linear baseband model, begins with the loop shown in Figure 1. The received signal is

$$r(t)=\sqrt{\frac{2E_s}{T}}\cos\left(\omega_c t-\theta_m+\theta_i\right)+w(t) \qquad (1)$$

where $w(t)$ is additive white gaussian noise with PSD $N_o/2$. The VCO output is $\sin\left(\omega_c t+\theta_o\right)$. The integrator outputs are

$$\begin{aligned} I &= I_s+N_i=\cos\left(\phi-\theta_m\right)+N_i \\ Q &= Q_s+N_q=-\sin\left(\phi-\theta_m\right)+N_q \end{aligned} \qquad (2)$$

with $g=\sqrt{\frac{2}{TE_s}}$ and phase error

$$\phi=\theta_i-\theta_o. \qquad (3)$$

This phase error is relative to the lock point and takes on values in the interval $(\pi/M,-\pi/M)$. The integrator gain term infers that ideal automatic gain control (AGC) is assumed.

0-7803-0953-7/93$03.00 © 1993 IEEE

The error signal is

$$\varepsilon(t) = I\hat{Q} - Q\hat{I}. \tag{4}$$

Substituting (2) into (4) results in

$$\begin{aligned}\varepsilon(t) &= \cos(\phi - \theta_m)\hat{Q} + N_I\hat{Q} \\ &\quad -\left(-\sin(\phi - \theta_m)\right)\hat{I} - N_Q\hat{I}.\end{aligned} \tag{5}$$

Neglecting noise and assuming good data decisions yields the expected mixer-type phase detector characteristic:

$$\begin{aligned}\varepsilon'(t) &= \cos(\phi)\left(I_m\hat{Q} - Q_m\hat{I}\right) \\ &\quad + \sin(\phi)\left(Q_m\hat{Q} + I_m\hat{I}\right) = \sin(\phi).\end{aligned} \tag{6}$$

Writing the error signal as its expected value plus noise,

$$\varepsilon(t) = E[\varepsilon(t)] + N_e(t) = PD(\phi) + N_e(t) \tag{7}$$

it is noted that the error signal is made up of the phase detector characteristic term and an equivalent noise term where

$$N_e(t) = N_I\hat{Q} - N_Q\hat{I} \tag{8}$$

and $$E[\varepsilon(t)] = E\left[\sin\left(\phi + \hat{\theta}_m - \theta_m\right)\right]. \tag{9}$$

The expected value of the error signal, the phase detector characteristic, can be expressed as

$$PD(\phi) = \alpha_{SNR}\sin(\phi) \tag{10}$$

where α_{SNR} is the amplitude suppression factor. It is defined by

$$\alpha_{SNR} = \left.\frac{\partial PD(\phi)}{\partial\phi}\right|_{\phi=0}. \tag{11}$$

With the error signal defined as in (7) a baseband model is readily available. Further, a linear baseband model, necessary for continuing the analysis, is available by assuming the phase error is small. The linear baseband model for a second-order high SNR MAP loop is shown in Figure 2.

The transfer function from the equivalent noise port to the VCO output port is

$$H_N(s) = \frac{K_v(s+a)}{s^2 + \alpha_{SNR}K_v(s+a)} = \frac{1}{\alpha_{SNR}}H(s) \tag{12}$$

where

$$H(s) = \frac{\alpha_{SNR}K_v(s+a)}{s^2 + \alpha_{SNR}K_v(s+a)}. \tag{13}$$

Expressing (13) in terms of the classical second-order control loop design parameters results in

$$H(s) = \frac{2\zeta'\omega_n's + \omega_n'^2}{s^2 + 2\zeta'\omega_n's + \omega_n'^2} \tag{14}$$

where

$$\begin{aligned}\omega_n' &= \sqrt{\alpha_{SNR}}\sqrt{K_v a} = \sqrt{\alpha_{SNR}}\omega_n \\ \zeta' &= \sqrt{\alpha_{SNR}}\frac{1}{2}\sqrt{\frac{K_v}{a}} = \sqrt{\alpha_{SNR}}\zeta.\end{aligned} \tag{15}$$

The variance of the phase error is found by considering the relationship between the input and output PSD's of the linear system, $\frac{1}{\alpha_{SNR}}H(s)$, where

$$S_{\theta_o}(\omega) = S_{N_e}(\omega)\left(\frac{1}{\alpha_{SNR}^2}\right)\left|H(j\omega)\right|^2 \tag{16}$$

and $$S_{N_e}(\omega) = \int_{-\infty}^{\infty} R_{N_e}(\tau)e^{-j\omega\tau}d\tau. \tag{17}$$

Since $N_e(t)$ is cyclostationary with period T its PSD is given by [3]

$$S_{N_e}(\omega) = \sigma_{N_e}^2 T\,\mathrm{sinc}^2\left(\frac{\omega T}{2\pi}\right). \tag{18}$$

The variance of the phase error can be expressed as

$$\sigma_{\theta_o}^2 = \frac{1}{\alpha_{SNR}^2}\frac{1}{2\pi}\int_{-\infty}^{\infty} S_{N_e}(\omega)\left|H(j\omega)\right|^2 d\omega. \tag{19}$$

Noting that the loop noise BW is much smaller than the BW of the equivalent noise, (19) becomes

$$\sigma_{\theta_o}^2 = \frac{1}{\alpha_{SNR}^2}\frac{\sigma_{N_e}^2}{\frac{1}{T}}\frac{1}{2\pi}\int_{-\infty}^{\infty}\left|H(j\omega)\right|^2 d\omega \tag{20}$$

where $\frac{1}{T} = SR$, the symbol rate. Noting that the integral in (20) is the two-sided loop BW, B_L, the variance becomes

$$\sigma^2_{\theta_o} = \frac{B_L}{SR}\frac{\sigma^2_{N_e}}{\alpha^2_{SNR}}. \quad (21)$$

What remains is to evaluate the three varying components of the phase error variance, B_L, $\sigma^2_{N_e}$, and α_{SNR}.

The Equivalent Noise Variance

To calculate $\sigma^2_{N_e}$, the equivalent noise variance, it is first noted that $E[N_e(t)] = 0$. Therefore, using (8), the variance is

$$\sigma^2_{N_e} = E[N_e(t)^2] = E[N_I^2\hat{Q}^2 + N_Q^2\hat{I}^2 - 2N_IN_Q\hat{I}\hat{Q}]. \quad (22)$$

For BPSK, with data on the I-channel, (22) reduces to

$$\sigma^2_{N_e} = E[N_Q^2] = \sigma^2_{N_Q} \quad (23)$$

which is the noise variance out of the quadrature correlator and can be expressed as

$$\sigma^2_{N_e} = \sigma^2_{N_I} = \frac{N_o}{2E_s}. \quad (24)$$

For QPSK (22) is expanded using the I and Q channel independence of noise and data resulting in

$$\sigma^2_{N_e} = E[N_I{}^2]E[\hat{Q}^2] + E[N_Q{}^2]E[\hat{I}^2] + E[-2N_QN_I\hat{I}\hat{Q}]. \quad (25)$$

With algebraic manipulation (25) reduces to

$$\sigma^2_{N_e} = \frac{N_o}{2E_s} - 2\{E[N_I\hat{I}]\}^2 \quad (26)$$

where

$$E[N_I\hat{I}] = \int_{-\infty}^{\infty}\int_{-\infty}^{\infty} N_I\hat{I}f(N_I)f(I_m)dN_IdI_m, \quad (27)$$

$$f(N_I) = \frac{1}{\sqrt{2\pi}\sigma_{N_I}}e^{-\frac{N_I^2}{2\sigma^2_{N_I}}}, \text{ and} \quad (28)$$

$$f(I_m) = \frac{1}{2}\delta\left(I_m - \frac{\sqrt{2}}{2}\right) + \frac{1}{2}\delta\left(I_m + \frac{\sqrt{2}}{2}\right). \quad (29)$$

Performing the indicated integration of (27) over the possible transmitted symbols and the noise, and then substituting the result into (26) yields

$$\sigma^2_{N_e} = \frac{N_0}{2E_s} - 2\left\{\frac{\sigma_{N_I}}{\sqrt{\pi}}e^{-\frac{1}{4\sigma^2_{N_I}}}\right\}^2 = \frac{N_0}{2E_s}\left(1 - \frac{2}{\pi}e^{-\frac{E_s}{N_0}}\right). \quad (30)$$

For 8 and 16-PSK the variance calculation of the equivalent noise cannot be reduced using the I and Q channel independence of noise and data and so must be calculated directly

$$\sigma^2_{N_e} = \int_{-\infty}^{\infty}\int_{-\infty}^{\infty}\int_{-\infty}^{\infty}\begin{bmatrix} g(N_I,N_Q,\theta_m) \\ \times f(N_Q,N_I,\theta_m) \\ \times dN_QdN_Id\theta_m \end{bmatrix} \quad (31)$$

where $g(N_I,N_Q,\theta_m)$ is the square of the equivalent noise and $f(N_Q,N_I,\theta_m)$ is the joint density on noise and the transmitted phase angle. With the use of numerical integration (31) can be calculated. The results for 8 and 16 PSK are shown in Figure 3 along with the analytical solutions for BPSK and QPSK. It is apparent from an examination of the results that for M>2 the equivalent noise variance approaches that of BPSK at high SNR. In fact, at SNR's that would be considered operational (E_s / N_o > 5 dB) this data suggests that the use of the BPSK solution is adequate.

At a given SNR the separation between the BPSK solution and any of the other variance curves is referred to as "self noise". Self noise reflects the fact that making bad data decisions has a small beneficial effect on how the noise effects the variance of the phase error.

The Amplitude Suppression Factor

The performance of the phase detector is degraded by making bad data decisions. This can be seen by examining the expected value of the error signal in (9). Similarly, this degradation appears as an amplitude suppression factor of the phase detector characteristic in (10). The amplitude suppression factor can be found from the phase detector characteristic by evaluating its derivative with respect to phase error when the phase error is zero, as described in (11). The factor itself is nothing more than the slope of the characteristic with zero phase error. As will be shown, an alternate method for obtaining the suppression factor

is to directly compute the slope of the characteristic. This is done by making use of the fact that the characteristic is linearly increasing for small phase errors. To proceed, the phase detector characteristic is written as an expected value of a function of two discrete random variables

$$PD(\phi)=\sum_{i=0}^{M-1}\sum_{j=0}^{M-1}\left[\begin{array}{l}\sin\left(\phi+\hat{\theta}_{m_j}-\theta_{m_i}\right)\\ \times P\left(\theta_{m_i},\hat{\theta}_{m_j}\right)\end{array}\right]. \quad (32)$$

Expanding the mutual probability results in

$$PD(\phi)=\sum_{i=0}^{M-1}\sum_{j=0}^{M-1}\left[\begin{array}{l}\sin\left(\phi+\hat{\theta}_{m_j}-\theta_{m_i}\right)\\ \times P\left(\hat{\theta}_{m_j}\middle|\theta_{m_i}\right)\\ \times P\left(\theta_{m_i}\right)\end{array}\right]. \quad (33)$$

Since all of the transmitted symbols are equiprobable if the modulation angle is set to zero, i.e., $\theta_m=0$, then (33) reduces to

$$PD(\phi)=\sum_{j=0}^{M-1}\sin\left(\phi+\hat{\theta}_{m_j}\right)P\left(\hat{\theta}_{m_j}\middle|\theta_m=0\right). \quad (34)$$

The conditional probability in (34) can be found from the probability density function that describes the probability of receiving a particular phase, γ, given $\theta_m=0$ and ϕ [4]:

$$p\left(\gamma|\theta_m=0,\phi\right)=\frac{1}{2\pi}e^{-\frac{E_s}{N_o}}\times\left\{1+\left[\begin{array}{l}\sqrt{\frac{4E_s\pi}{N_o}}\cos(\gamma+\phi)\\ \times e^{-\left(\frac{E_s}{N_o}\cos(\gamma+\phi)^2\right)}\end{array}\right]Q\left(-\sqrt{\frac{2E_s}{N_o}}\cos(\gamma+\phi)\right)\right\} \quad (35)$$

where $Q(x)$ is the complementary error function. To calculate $P\left(\hat{\theta}_{m_j}\middle|\theta_m=0\right)$, (35) is integrated over the decision region that corresponds to $\hat{\theta}_{m_i}$. The 8PSK phase detector characteristics for three SNR's are shown in Figure 4. The degrading effect of the amplitude suppression factor on the phase detector characteristic, which increases with decreasing SNR, is apparent. From this data the amplitude suppression factor can be easily calculated. By computing the slope between two points from the phase detector characteristic data, one on either side of and very close to the $\phi=0$ point, the amplitude suppression factor can be computed for any M, at any SNR.

Loop Noise Bandwidth

The final component necessary for computing the phase error variance is the loop noise bandwidth, B_L. Using the definition for the loop noise bandwidth of a second order loop with a perfect integrator, and noting the natural frequency and damping factor parameter definitions of (15), B_L can be expressed as

$$B_L=\omega_n\left(\alpha_{SNR}\zeta+\frac{1}{4\zeta}\right). \quad (36)$$

Figure 5 shows the effect of changing SNR on the loop noise bandwidth. Note that this is not the result of changing signal level, i.e., we have assumed ideal AGC, but rather the effect of incorrect data decisions on the phase detector. The "design" BW (the high SNR BW) corresponds to a normalized loop BW of 1. As the SNR decreases, the amplitude suppression factor decreases. This narrows the loop noise bandwidth.

Assembling The Variance Of The Phase Error

Restating (21)

$$\sigma_{\theta_o}^2=\frac{B_L}{SR}\frac{\sigma_{N_e}^2}{\alpha_{SNR}^2} \quad (37)$$

and considering that the equivalent noise variance can be written as

$$\sigma_{N_e}^2=\frac{N_o}{2E_s}\xi_{SNR} \quad (38)$$

where ξ_{SNR} is the self noise, the variance of the phase error can be expressed as

$$\sigma_{\theta_o}^2=\frac{N_o}{2E_s}\frac{B_L}{SR}\frac{\xi_{SNR}}{\alpha_{SNR}^2}. \quad (39)$$

The quotient $\frac{\alpha_{SNR}^2}{\xi_{SNR}}$ is often referred to as the "squaring" loss or, more appropriately, the "n-phase" loss and is denoted by SL. It reflects the increase in variance of the phase error that is imposed for tracking the double-sideband suppressed-carrier of an M-PSK signal as opposed to a continuous wave (CW) carrier. Since the

self noise is negligible for operational SNR's, it is convenient to write the n-phase loss as

$$SL = \frac{\alpha_{SNR}^2}{\xi_{SNR}} \approx \alpha_{SNR}^2 . \quad (40)$$

Figure 6 shows this approximation for the n-phase loss for MPSK. Note the difference in n-phase loss between BPSK or QPSK and 16PSK for higher SNR's. At an E_s / N_o of 10dB there is approximately 40 dB more variance in a 16PSK recovered carrier than in a BPSK or QPSK recovered carrier.

Variance Of Phase Error Results

Simulations were conducted to verify the analysis of the variance of the phase error. Using uncorrelated samples from a time simulation of the carrier tracking process, the variance of phase error was computed. The simulation data and analysis data for BPSK and QPSK are shown in Figure 7. For this data the ratio of loop noise BW to symbol rate at high SNR is 0.625%. To evaluate this data consider that a standard deviation in phase error of 1 degree corresponds to the -35 dB variance point on the graph. A 2 degree standard deviation corresponds to -29 dB and a 3 degree standard deviation corresponds to -26 dB. BPSK requires approximately 1 dB E_s / N_o to achieve the 3 degree standard deviation threshold. Similarly for QPSK an E_s / N_o of 4 dB is required to maintain this same threshold. To achieve the one degree threshold would require approximately 10 dB E_s / N_o for both BPSK and QPSK. At these SNR's it is also prudent to discuss the 3 dB "break-away" threshold for M > 2 (For BPSK this threshold occurs at a very low SNR). This threshold describes the point at which a 1 dB decrease in SNR will correspond to more than a 3 dB increase in variance of the phase error. From Figure 7 it is apparent that for QPSK the 3 dB threshold occurs at approximately 4 dB E_s / N_o.

The 8PSK data is presented in Figure 8. The two sets of curves correspond to two different ratios of loop noise BW to symbol rate at high SNR. The different ratios are 6 dB apart. It is important to note that the simulated and calculated data curves are not 6 dB apart at lower SNR's (in the neighborhood of the previously mentioned thresholds). The straight line approximations correspond to neglecting n-phase loss and are used to determine the 3 dB threshold which occurs at approximately 11 dB E_s / N_o for both sets of curves. The 1 degree thresholds for loop noise BW to symbol rate ratios of 0.125% and 0.5% occur at E_s / N_o's of approximately 9.5 dB and 11.5 dB respectively.

It should be noted that the difference in ratios of loop noise BW to symbol rate between the 8PSK data and that of BPSK and QPSK were needed to obtain simulation data at E_s / N_o's as low as 6 dB for 8PSK. The simulation data plotted for 8PSK, and in Figure 9 for 16PSK, reveal the lowest possible SNR's that could be used for obtaining variance data. Below the SNR's for which data is plotted in these curves, the simulator did not maintain lock. This lock threshold is much lower for BPSK and QPSK even at the wider loop ratio of 0.625% and in fact is not reflected by the data in Figure 7.

As expected, the 16PSK data shown in Figure 9 for a 0.125% ratio of loop noise BW to symbol rate at high SNR indicates even higher thresholds in SNR. The 1 degree threshold occurs at an E_s / N_o of approximately 14 dB. The 3 dB break-away threshold occurs at approximately 17 dB.

Conclusions

In practical BPSK and QPSK satellite modems a carrier phase jitter standard deviation of 1 degree is considered to be a good performance threshold since it will have a negligible effect on BER performance. Considering this specification the effects of n-phase loss and changing loop BW have been of little concern to the design engineer. However, if BW efficiency is to be increased through the use of coded systems such as 8 and 16 PSK TCM while maintaining other system specifications, e.g., SNR and loop noise BW to symbol rate ratio, this research suggests that degraded performance can be expected in the high SNR MAP estimation loop. Not only will there be a significant increase in carrier phase jitter due to data decision errors but the loop may not acquire and may not maintain lock at desired SNR's in the power-limited channel.

References

[1] W. Osborne and B. Kopp, "Synchronization in M-PSK Modems," *IEEE Int. Conf. Commun. Rec.*, pp. 348.6.1-348.6.5 ,1992.

[2] M. K. Simon, "Further Results on Optimum Receiver Structures for Digital Phase and Amplitude Modulated Signals," *Int. Conf. Commun. Rec.*, pp. 42.1.1-42.1.7, 1978.

[3] S. Hinedi and W. Lindsey, "On the Self-Noise in QASK Decision-Feedback Carrier Tracking Loops," *IEEE Trans. Commun.*, Vol. 37, April 1989.

[4] R. Parsons and S. Wilson., "Polar Quantizing for Coded PSK Transmission," *IEEE Trans. Commun.*, Vol. 38, Sept. 1990.

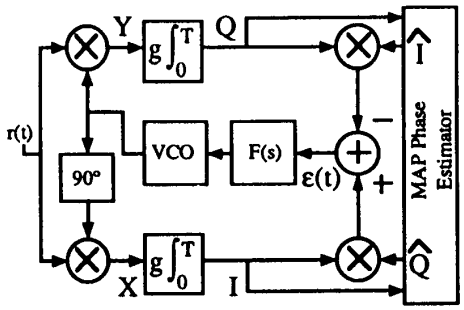

Figure 1. The M-PSK high SNR MAP receiver.

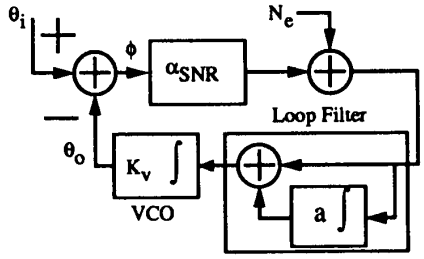

Figure 2. The linear baseband model.

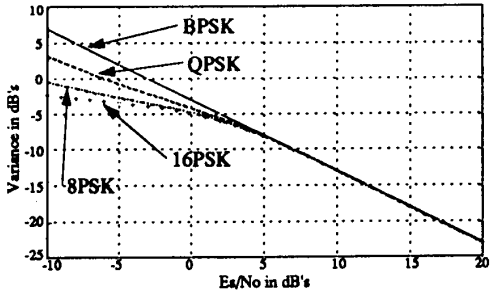

Figure 3. M-PSK equivalent noise variance.

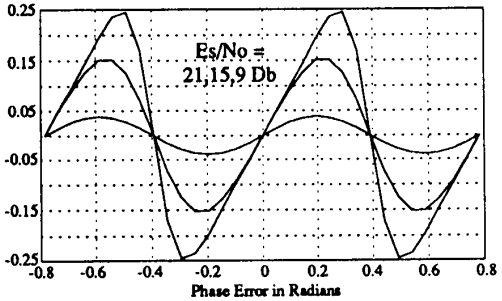

Figure 4. 8PSK phase detector characteristics.

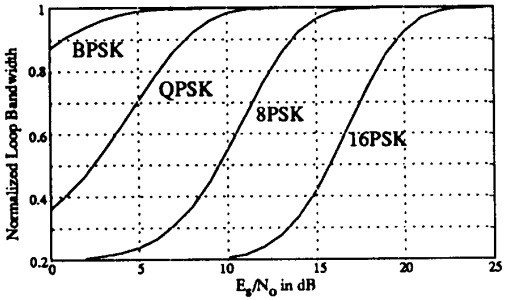

Figure 5. Normalized loop noise bandwidth.

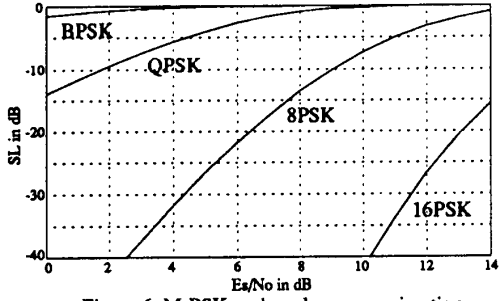

Figure 6. M-PSK n-phase loss approximation.

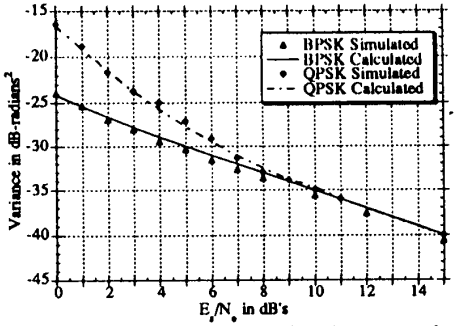

Figure 7. BPSK and QPSK carrier phase error data.

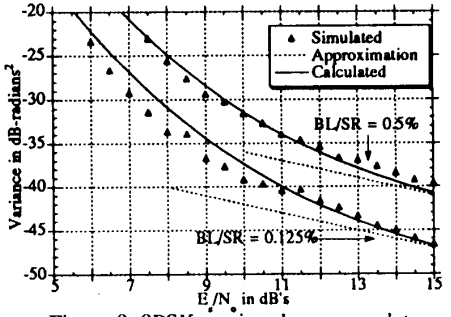

Figure 8. 8PSK carrier phase error data.

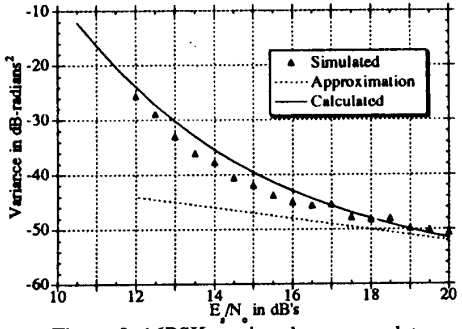

Figure 9. 16PSK carrier phase error data.